Diffuse attenuation coefficient of downwelling irradiance: An evaluation of remote sensing methods

Zhong-Ping Lee,[1,2] Miroslaw Darecki,[3] Kendall L. Carder,[4] Curtiss O. Davis,[5] Dariusz Stramski,[6] and W. Joseph Rhea[5]

Received 1 July 2004; revised 18 November 2004; accepted 28 December 2004; published 22 February 2005.

[1] The propagation of downwelling irradiance at wavelength λ from surface to a depth (z) in the ocean is governed by the diffuse attenuation coefficient, $\bar{K}_d(\lambda)$. There are two standard methods for the derivation of $\bar{K}_d(\lambda)$ in remote sensing, which both are based on empirical relationships involving the blue-to-green ratio of ocean color. Recently, a semianalytical method to derive $\bar{K}_d(\lambda)$ from reflectance has also been developed. In this study, using $\bar{K}_d(490)$ and $\bar{K}_d(443)$ as examples, we compare the $\bar{K}_d(\lambda)$ values derived from the three methods using data collected in three different regions that cover oceanic and coastal waters, with $\bar{K}_d(490)$ ranging from $\sim$0.04 to 4.0 m^{-1}. The derived values are compared with the data calculated from in situ measurements of the vertical profiles of downwelling irradiance. The comparisons show that the two standard methods produced satisfactory estimates of $\bar{K}_d(\lambda)$ in oceanic waters where attenuation is relatively low but resulted in significant errors in coastal waters. The newly developed semianalytical method appears to have no such limitation as it performed well for both oceanic and coastal waters. For all data in this study the average of absolute percentage difference between the in situ measured and the semianalytically derived $\bar{K}_d$ is $\sim$14% for λ = 490 nm and $\sim$11% for λ = 443 nm.

Citation: Lee, Z.-P., M. Darecki, K. L. Carder, C. O. Davis, D. Stramski, and W. J. Rhea (2005), Diffuse attenuation coefficient of downwelling irradiance: An evaluation of remote sensing methods, *J. Geophys. Res.*, *110*, C02017, doi:10.1029/2004JC002573.

1. Introduction

[2] For many oceanographic studies, the diffuse attenuation coefficient, $K_d(\lambda)$ (where λ is the light wavelength in free space), of the spectral solar downward irradiance, $E_d(\lambda)$, plays a critical role. These studies include the heat transfer in the upper ocean [*Chang and Dickey*, 2004; *Lewis et al.*, 1990; *Morel and Antoine*, 1994; *Zaneveld et al.*, 1981], photosynthesis and other biological processes in the water column [*Marra et al.*, 1995; *McClain et al.*, 1996; *Platt et al.*, 1988; *Sathyendranath et al.*, 1989], and turbidity of oceanic and coastal waters [*Jerlov*, 1976; *Kirk*, 1986].

[3] $K_d(\lambda)$ is an apparent optical property [*Preisendorfer*, 1976], so it varies to some extent with solar zenith angle, sky and surface conditions, as well as with depth even within the well mixed water column [*Gordon*, 1989; *Liu et al.*, 2002]. In ocean color remote sensing, the commonly used quantity is the vertically averaged value of $K_d(\lambda)$ in the surface mixed layer, denoted in this article as $\bar{K}_d(\lambda)$ or $\bar{K}_d$ for brevity. For the vast oceans, estimation of $\bar{K}_d(\lambda)$ of the surface layer by satellite remote sensing of ocean color (i.e., the spectral radiance of the ocean as seen by a radiance sensor deployed on satellite) is the only practical means to provide repetitive measurements over extended spatial and temporal scales.

[4] At present, two operational standard algorithms are used for the derivation of $\bar{K}_d(\lambda)$ in ocean color remote sensing. In method 1, $\bar{K}_d(490)$ ($\bar{K}_d$ at λ = 490 nm) is estimated from an empirical algorithm based on the relationship between $\bar{K}_d(490)$ and the blue-to-green ratio of water-leaving radiance, L_w, or remote sensing reflectance, R_{rs} [*Austin and Petzold*, 1981; *Mueller*, 2000]. This $\bar{K}_d(490)$ value can then be used to estimate $\bar{K}_d$ at other wavelengths from empirical relationships between $\bar{K}_d(490)$ and $\bar{K}_d(\lambda)$ [*Austin and Petzold*, 1986]. In method 2, chlorophyll *a* concentration (Chl) is first estimated from an empirical algorithm based on the blue-to-green ratio of R_{rs}. This Chl value is then used for the estimation of $\bar{K}_d(\lambda)$ based on another set of empirical relationships between $\bar{K}_d(\lambda)$ and Chl [*Morel*, 1988; *Morel and Maritorena*, 2001]. Recently, based on numerical simulations of radiative transfer in the ocean, a new semianalytical method (method 3) to calculate $\bar{K}_d(\lambda)$ from $R_{rs}(\lambda)$ has been developed [*Lee et al.*, 2005]. This method quasi-analytically derives the absorption and backscattering coefficients from $R_{rs}(\lambda)$; and then these coefficients are used as input to a semianalytical model to estimate the values of $\bar{K}_d(\lambda)$. All three methods appear quite

[1]Naval Research Laboratory, Stennis Space Center, Mississippi, USA.
[2]Also visiting professor at Ocean Remote Sensing Institute, Ocean University of China, Qingdao, China.
[3]Institute of Oceanology, Polish Academy of Sciences, Sopot, Poland.
[4]College of Marine Science, University of South Florida, St. Petersburg, Florida, USA.
[5]Naval Research Laboratory, Washington, DC, USA.
[6]Marine Physical Laboratory, Scripps Institution of Oceanography, University of California at San Diego, La Jolla, California, USA.

0148-0227/05/2004JC002573$09.00

promising but comprehensive tests with independent data obtained over a wide range of environmental conditions are critical for method validation and subsequent applications to world oceans.

[5] In this study, we examine the three methods using a large data set from field measurements taken in different regions that cover open ocean and coastal waters. For each method, using $\bar{K}_d(490)$ and $\bar{K}_d(443)$ as examples, we compare the $\bar{K}_d(\lambda)$ values estimated from in situ determinations of spectral L_w or R_{rs} with the $\bar{K}_d(\lambda)$ values obtained from in situ measurements of $E_d(\lambda, z)$ in the surface layer (z is the depth from surface). The performance of the three methods is compared.

2. Methods for Deriving $\bar{K}_d(\lambda)$ From Remote Sensing Measurements

[6] The three methods for estimating $\bar{K}_d(\lambda)$ from remote sensing reflectance are presented schematically in Figure 1. Below we describe the methods in greater detail.

2.1. Method 1: Direct One-Step Empirical Relationship for $\bar{K}_d(490)$

[7] In the approach developed by *Austin and Petzold* [1981, 1986], $\bar{K}_d(490)$ is the key for estimating $\bar{K}_d$ at other wavelengths. Pioneered by *Austin and Petzold* [1981], the simplest method to estimate $\bar{K}_d(490)$ is the empirical relation between $\bar{K}_d(490)$ and the ratio of water-leaving radiances at two wavelengths within the blue-green spectral region:

$$\bar{K}_d(490) = K_w(490) + A\left(\frac{L_w(\lambda_1)}{L_w(\lambda_2)}\right)^B. \quad (1)$$

In *Austin and Petzold* [1981], $\lambda_1 = 443$ nm and $\lambda_2 = 550$ nm. $K_w(490)$ is the attenuation coefficient associated with pure seawater [*Austin and Petzold*, 1981; *Morel*, 1988; *Smith and Baker*, 1981], and A and B are algorithm constants. Recently, for the purpose of estimating $\bar{K}_d(490)$ from Sea-Viewing Wide Field-of-View Sensor (SeaWiFS) on the OrbView-2 satellite, *Mueller and Trees* [1997] and *Mueller* [2000] proposed the following algorithm for SeaWiFS:

$$\bar{K}_d(490) = K_w(490) + 0.15645\left(\frac{L_w(490)}{L_w(555)}\right)^{-1.5401}, \quad (2)$$

with $K_w(490)$ of 0.016 m^{-1} performing the best for their data set [*Mueller*, 2000].

[8] Because remote sensing reflectance, R_{rs}, is defined as the ratio of water-leaving radiance to downwelling irradiance just above the surface, equation (2) can be written as

$$\bar{K}_d(490) = 0.016 + 0.15645\left(\frac{E_d(490)}{E_d(555)}\frac{R_{rs}(490)}{R_{rs}(555)}\right)^{-1.5401}. \quad (3)$$

Note that $E_d(490)/E_d(555)$ at the surface varies only slightly around 1.03 for different sun angles. In this study we use the constant $E_d(490)/E_d(555) = 1.03$ in equation (3) for estimating $\bar{K}_d(490)$ from in situ measurements of R_{rs}. Rewrite of equation (2) to equation (3) is simply for internal consistency among the methods that all use R_{rs} values as inputs.

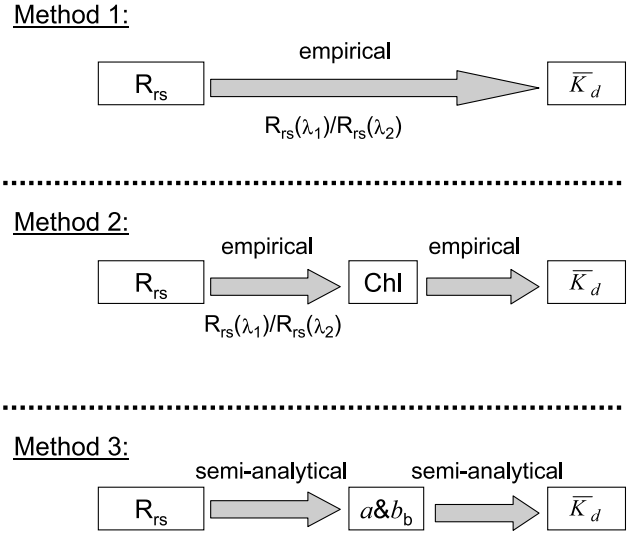

Figure 1. Schematic of the methods for estimating $\bar{K}_d$ from R_{rs}.

2.2. Method 2: Two-Step Empirical Algorithm With *Chl* as an Intermediate Link

[9] Another commonly applied approach is to first derive chlorophyll *a* concentration, Chl, from remote sensing reflectance using an empirical algorithm [*O'Reilly et al.*, 1998], and then to derive $\bar{K}_d(\lambda)$ from Chl using another set of empirical relationships [*Morel*, 1988; *Morel and Maritorena*, 2001]. The current operational Chl algorithm for SeaWiFS (OC2v4) (see http://seawifs.gsfc.nasa.gov/SEAWIFS/RECAL/Repro3/OC4_reprocess.html),

$$\mathrm{Chl} = 10^{a_0 + a_1\rho + a_2\rho^2 + a_3\rho^3} + a_4, \quad (4)$$

is here applied for the derivation of Chl from remote sensing reflectance, where $\rho = \log_{10}[R_{rs}(490)/R_{rs}(555)]$. The values of a_0, a_1, a_2, a_3, and a_4 are 0.319, −2.336, 0.879, −0.135, and −0.071, respectively, which were derived statistically from pooled field data collected in various parts of the oceans (see http://seawifs.gsfc.nasa.gov/SEAWIFS/RECAL/Repro3/OC4_reprocess.html).

[10] From another set of field measurements, empirical relationships between $\bar{K}_d(\lambda)$ and Chl were developed [*Morel*, 1988; *Morel and Maritorena*, 2001]:

$$\bar{K}_d(\lambda) = K_w(\lambda) + \chi(\lambda)\,\mathrm{Chl}^{e(\lambda)}, \quad (5)$$

where the values of $K_w(\lambda)$, $\chi(\lambda)$ and $e(\lambda)$ result from statistical analysis of the data [see *Morel and Maritorena*, 2001, Table 2]. For $\lambda = 490$ nm, K_w, χ, and e are 0.0166 m^{-1}, 0.07242, and 0.68955, respectively. When the ratio of $R_{rs}(490)/R_{rs}(555)$ is provided from field or satellite measurements, $\bar{K}_d(\lambda)$ can be readily calculated from equations (4) and (5). Clearly, for both method 1 and method 2, the inputs for calculation of $\bar{K}_d(\lambda)$ are exactly the same in this study.

2.3. Method 3: Semianalytical Approach

[11] Method 3 involves the concept that the apparent optical properties of the ocean are determined by the inherent optical properties of seawater and boundary conditions (such as solar zenith angle and sea state) through radiative transfer theory [*Gordon et al.*, 1975]. In this strategy, the values of the absorption, a, and backscattering, b_b, coefficients are most essential to the determination of both apparent optical properties of interest to our study, R_{rs} and $\bar{K}_d$ (wavelength notation suppressed). When the values of a and b_b are known, along with boundary conditions, R_{rs} and $\bar{K}_d$ can be calculated from semianalytical models [*Lee et al.*, 2004, 2005; *Sathyendranath and Platt*, 1997]. In remote sensing applications by satellite imagery, R_{rs} is determined from satellite measurements. The solar zenith angle is also known for each pixel of the image. Thus the first step is to derive a and b_b from R_{rs}, and then the second step is to calculate $\bar{K}_d$ from these a and b_b values.

[12] For the first step, *Lee et al.* [2002] have developed a Quasi-Analytical Algorithm (QAA) which is briefly described in Appendix A. For the second step, *Lee et al.* [2005] refined the simple $\bar{K}_d$ formula of *Sathyendranath et al.* [1989] to improve the quantification of the contribution associated with the backscattering coefficient,

$$\bar{K}_d = m_0 a + m_1(1 - m_2 e^{-m_3 a})b_b, \tag{6}$$

where $m_0 \approx 1 + 0.005\theta_a$ and θ_a is the solar zenith angle in air. The values for model constants m_1, m_2, and m_3 are 4.18, 0.52, and 10.8, respectively [*Lee et al.*, 2005]. These values remain constant for different waters and different wavelengths. As stated earlier and shown by equation (6), $\bar{K}_d$ varies with both a and b_b, as well as with solar zenith angle. Note that a and b_b change with water mass and wavelength. A short description regarding this semianalytical model is provided in Appendix B. The essence of method 3 is that $\bar{K}_d$ can be easily calculated based on the QAA and equation (6) when the values of $R_{rs}(\lambda)$ are known.

[13] Compared to method 1 and method 2, method 3 is more complex due to its semianalytical nature. Both method 1 and method 2 are data-driven empirical algorithms and their performance may be subject to large errors, especially when the data used in the algorithm development do not match the data under study [*Darecki and Stramski*, 2004]. For such empirical algorithms, it is difficult to apply the same procedures globally. The semianalytical approach, however, follows in principle the radiative transfer theory, so it has fewer uncertainties regarding data matching. On the other hand, method 3 uses not only the spectral shape but also the values of R_{rs} to derive a and b_b and then $\bar{K}_d$, so accurate measurements of R_{rs} are important.

[14] In the QAA inversion of R_{rs} to yield a and b_b [*Lee et al.*, 2002], the use of a reference wavelength around 640 nm is required to improve accuracy in coastal waters. In the current satellite ocean color sensors such as SeaWiFS or MODIS (Moderate Resolution Imaging Spectroradiometer), no spectral band in the vicinity of 640 nm is designed for ocean applications. In order to apply this semianalytical approach to data from these satellite sensors, an empirical scheme to simulate a measurement at 640 nm from measurements at current SeaWiFS (or MODIS) wavelengths was developed (Z. P. Lee and K. L. Carder, unpublished data, 2002):

$$R_{rs}(640) = 0.01R_{rs}(555) + 1.4R_{rs}(667) - 0.0005R_{rs}(667)/R_{rs}(490). \tag{7}$$

This empirical relationship was developed based on field measurements made in the Gulf of Mexico in 1999 and 2000, which are independent of the data sets utilized in this study.

3. Data

[15] Field measurements from three different regions are used for testing and evaluating the three methods for estimating $\bar{K}_d$. The regions are: the Gulf of Mexico (data collected in April 1993), the Arabian Sea (December 1994), and the Baltic Sea (1993–2001). These regions include open ocean oligotrophic waters (the Loop Current, and Arabian Sea), near-shore high-productivity waters (the West Florida Shelf), and relatively turbid coastal waters of the shallow intracontinental sea (Baltic). The range of chlorophyll concentration was $\sim$0.09–100 mg m^{-3} with $\bar{K}_d(490)$ ranging from $\sim$0.04 to 4.0 m^{-1}. These measurements were taken with a solar zenith angle (θ_a) between 20° and 80° under both clear skies and the Sun covered by clouds. For the conditions with the Sun covered by clouds, θ_a is taken as 45° as by *Sathyendranath et al.* [1989].

[16] Detailed description of the experimental work, the investigated waters, and environmental conditions can be found elsewhere [*Darecki and Stramski*, 2004; *Lee et al.*, 1996]. Briefly, in the Gulf of Mexico and the Arabian Sea, $R_{rs}(\lambda)$ was calculated from measurements made above the sea surface as described by *Carder and Steward* [1985], with upwelling radiance, downwelling irradiance, and downwelling sky radiance measured by a custom-made, handheld spectroradiometer. The methodology for determining $R_{rs}(\lambda)$ is also described in detail in NASA protocol [*Mueller et al.*, 2002]. For the Baltic Sea, $R_{rs}(\lambda)$ was calculated based on vertical profiles of $L_u(\lambda, z)$ (the spectral upwelling radiance at depth z) and $E_d(\lambda, z)$ (the spectral downwelling irradiance at depth z). These quantities were measured with a MER2040 spectroradiometer (Biospherical Instruments, Inc.) (*see Darecki and Stramski* [2004] for details). For each station reported in this study, $\bar{K}_d(\lambda)$ within the surface layer was calculated from the vertical profiles of $E_d(\lambda, z)$, following the approach of *Smith and Baker* [1981]. Specifically, $\bar{K}_d(\lambda)$ is the slope of the linear regression between z and $\ln[E_d(\lambda, z)]$.

4. Results and Discussion

[17] To demonstrate the performance of the three methods, we present results for $\bar{K}_d(490)$ and $\bar{K}_d(443)$. The $\bar{K}_d(\lambda)$ values determined from the measured profiles of $E_d(\lambda, z)$ will be referred to as $\bar{K}_d^{\text{mea}}$, and the $\bar{K}_d(\lambda)$ values derived from $R_{rs}(\lambda)$ using any of the three methods will be referred to as $\bar{K}_d^{\text{der}}$. To quantify the differences between $\bar{K}_d^{\text{mea}}$ and

Table 1. Evaluation of R_{rs}-Derived $\bar{K}_d$ Values Versus $\bar{K}_d$ Values From the $E_d(z)$ Measurements[a]

	Method 1	Method 2	Method 3
$\bar{K}_d(490)$ (0.04–4.0 m^{-1})			
apd	0.440	0.633	0.141
R^2	0.680	0.538	0.911
Intercept	0.140	0.071	0.011
Slope	0.316	0.412	0.880
$\bar{K}_d(443)$ (0.04–5.0 m^{-1})			
apd	0.577	0.916	0.112
R^2	0.679	0.555	0.885
Intercept	0.199	0.089	−0.005
Slope	0.305	0.371	1.059
N	**875**	**875**	**875**

[a] R^2 (square of correlation coefficient), intercept, and slope are results from analysis by linear regression.

$\bar{K}_d^{\text{der}}$, average of the absolute percentage difference (apd) is calculated after log transformation:

$$\text{apd} = \exp\left(\text{mean}\left|\ln\left(\frac{\bar{K}_d^{\text{der}}}{\bar{K}_d^{\text{mea}}}\right)\right|\right) - 1. \quad (8)$$

In equation (8), an equal weighting is placed on the percentage difference for over- and underestimates of $\bar{K}_d$ values.

[18] Table 1 summarizes the apd values for the three methods investigated, along with the results of linear regression analysis. For guidance regarding algorithm performance, a perfect match between $\bar{K}_d^{\text{mea}}$ and $\bar{K}_d^{\text{der}}$ should have apd = 0, R^2 = 1, intercept = 0, and slope = 1. Clearly, none of the methods examined exhibits these ideal values, but method 3 has results that are much better than the two empirical methods.

4.1. $\bar{K}_d(490)$

[19] For $\bar{K}_d(490)$ [$\equiv\bar{K}_d^{\text{mea}}(490)$] covering a range of ~0.04–4.0 m^{-1} (a total of 875 points after excluding 12 points with questionable values of the measured $\bar{K}_d$ or R_{rs}), the apd values are 0.440 and 0.633 for methods 1 and 2, respectively. In analysis of linear regression, the slope is 0.316 (intercept = 0.140 m^{-1}) for method 1 and 0.412 (intercept = 0.071 m^{-1}) for method 2. These numbers suggest that both methods significantly and systematically underestimate $\bar{K}_d$ at relatively high $\bar{K}_d$ values, and slightly overestimate $\bar{K}_d$ at low $\bar{K}_d$ values.

[20] The underestimation is clearly shown in Figures 2 and 3, where Figure 2 compares $\bar{K}_d^{\text{der}}$ derived from $R_{rs}(\lambda)$ with $\bar{K}_d^{\text{mea}}$ obtained from the $E_d(z)$ measurements. Figure 3 presents the ratio of $\bar{K}_d^{\text{der}}$ to $\bar{K}_d^{\text{mea}}$, which illustrates how close the two sets of values are. For data with $\bar{K}_d(490)$ < ~0.2 m^{-1} (oceanic waters are usually in this range), it appears that both method 1 and method 2 produced reasonable estimates of $\bar{K}_d(490)$, although method 2 seems to perform slightly better than method 1. For $\bar{K}_d(490)$ > ~0.2 m^{-1}, however, both empirical methods systematically and significantly underestimate $\bar{K}_d(490)$, as indicated by their slopes of 0.316 and 0.412 (Table 1). For this data set, only 44% of the $\bar{K}_d^{\text{der}}$ values at 490 nm derived by method 1 falls within ±25% of $\bar{K}_d^{\text{mea}}$, and 22% for method 2 (see Figures 3a and 3b). Most of the larger differences occur for waters with $\bar{K}_d(490)$ > ~0.2 m^{-1}, an upper limit for application of both methods.

[21] In addition to measurement errors that are unavoidable in any field-measured data, other fundamental factors can contribute to the disappointing performance of these methods. First, method 1 and method 2 are data-driven empirical algorithms. The algorithm coefficients contained

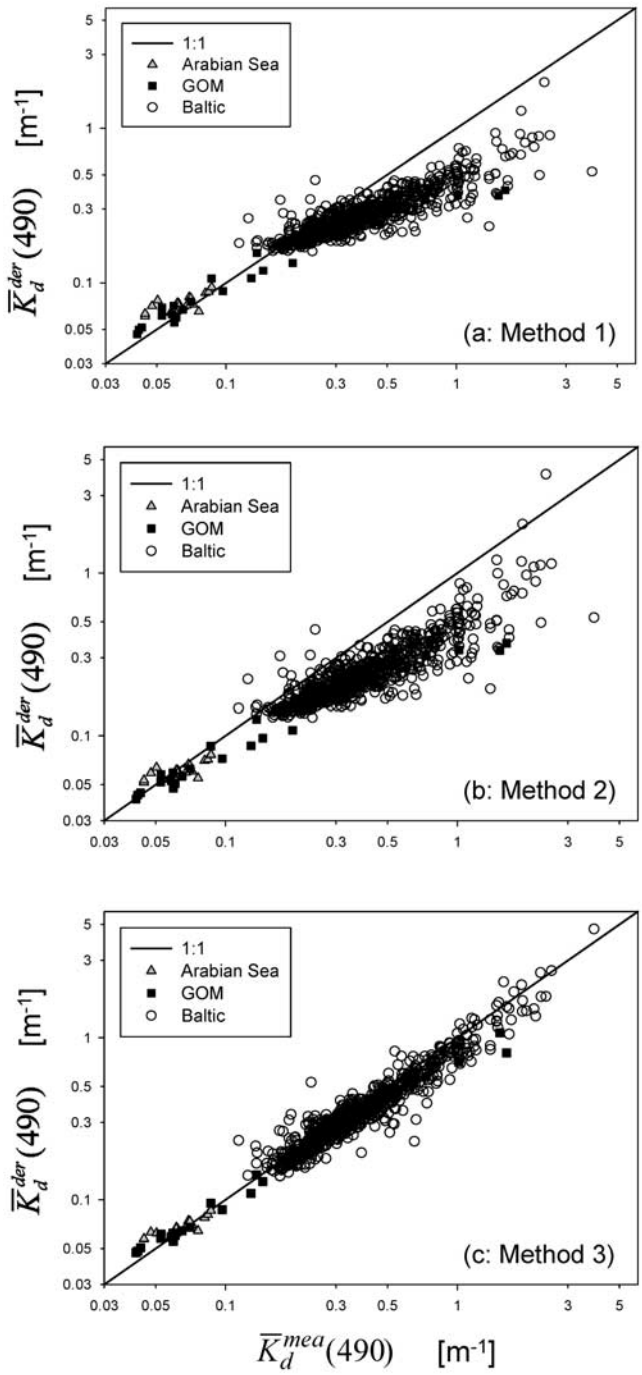

Figure 2. Algorithm-derived $\bar{K}_d^{\text{der}}(490)$ (i.e., R_{rs}-derived $\bar{K}_d(490)$) versus measured $\bar{K}_d^{\text{mea}}(490)$ (i.e., $E_d(490, z)$-derived $\bar{K}_d(490)$) in a log-log scale for measurements made in three regions as indicated (GOM, Gulf of Mexico; see text for more details) for (a) method 1, (b) method 2, and (c) method 3.

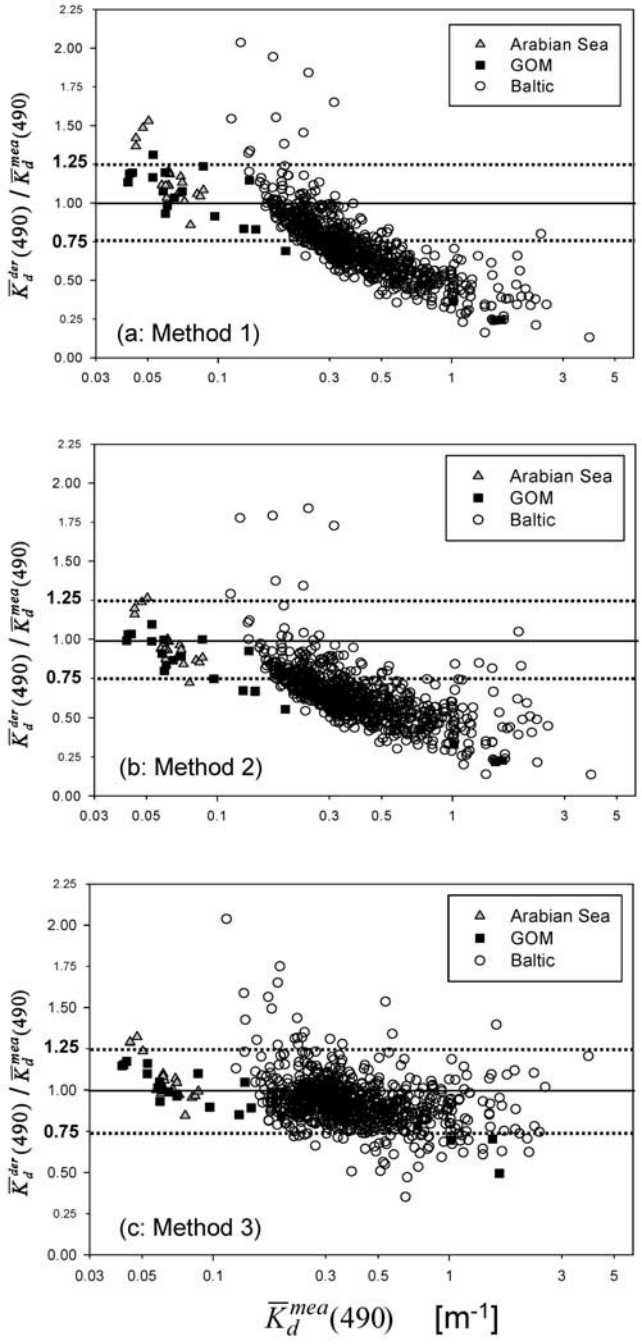

Figure 3. Ratio of algorithm-derived $\bar{K}_d^{\mathrm{der}}(490)$ to measured $\bar{K}_d^{\mathrm{mea}}(490)$ versus measured $\bar{K}_d^{\mathrm{mea}}(490)$, which illustrates how close the two quantities are for (a) method 1, (b) method 2, and (c) method 3.

in each of these methods are highly dependent upon the data set that was used for the algorithm development [*Mueller*, 2000]. Specifically, algorithm constants contained in method 1 were developed with most of the $\bar{K}_d(490)$ values being smaller than 0.25 m^{-1} [*Mueller*, 2000]. Also, the empirical coefficients of the relation between $\bar{K}_d(490)$ and Chl in method 2 were obtained using data with Chl < 2.4 mg m^{-3} [see *Morel and Maritorena*, 2001, Table 1], which implies a data range of $\bar{K}_d(490) < \sim 0.15$ m^{-1} according to equation (5).

[22] In the data set examined here, however, most of the data points (89% of all points shown) are for $\bar{K}_d(490) > 0.2$ m^{-1}. Therefore there is a big mismatch between data for algorithm development and data used in the algorithm evaluation. The performance of such data-driven algorithms for this data set is thus expected to be problematic. Tuning the algorithm coefficients to fit a data set covering a wider dynamic range in a given region is a way to remedy this limitation, at least to some extent [*Darecki and Stramski*, 2004]. However, such tuning approach does not guarantee a successful performance in general applications, and it does not provide an understanding of the mechanisms responsible for variability in the relationships between the diffuse attenuation coefficient and remote sensing reflectance.

[23] Second, in essence, $\bar{K}_d(490)$ from both method 1 and method 2 are derived from the ratio of $R_{rs}(490)/R_{rs}(555)$, with the actual magnitude of $R_{rs}(\lambda)$ being unimportant. Note that $\bar{K}_d$ is determined by both absorption and backscattering coefficients [*Gordon*, 1989; *Lee et al.*, 2005; *Sathyendranath et al.*, 1989; *Smith and Baker*, 1981]. However, the $R_{rs}(490)/R_{rs}(555)$ ratio is mainly a measure of the change in the absorption coefficient of water, whereas the change in the backscattering coefficient of water has generally a much smaller effect [*Carder et al.*, 1999; *Reynolds et al.*, 2001; *Stramska et al.*, 2003]. Thus it is clear that these traditional methods accounted mainly for the absorption part of $\bar{K}_d$ by employing only the spectral ratios of $R_{rs}(\lambda)$, and will work fine only for waters for which the effects of backscattering coefficients are significantly smaller than those of absorption coefficients.

[24] Third, the empirical algorithms suffer from the fact that the spectral ratio of $R_{rs}(490)/R_{rs}(555)$ approaches an asymptotic value with increasing concentration of optically significant water constituents [*Lee and Carder*, 2000]. Therefore this ratio is no longer sensitive to the variation of $\bar{K}_d(490)$ when $\bar{K}_d(490)$ is large, which results in significant underestimation of $\bar{K}_d$ for large $\bar{K}_d(490)$ values (see Figures 2a and 2b).

[25] Finally, although the diffuse attenuation coefficient is an apparent optical property (AOP) that varies with Sun angle [*Gordon*, 1989; *Liu et al.*, 2002], the expressions of equation (3) or equation (5) do not account for that source of variability in some well-defined systematic fashion. Because the ratio of $R_{rs}(490)/R_{rs}(555)$ or other spectral ratios of $R_{rs}(\lambda)$ are not sensitive to Sun angle variation [*Du et al.*, 2005; *Morel and Gentili*, 1993], the difference between $\bar{K}_d(490)$ derived from the $R_{rs}(\lambda)$ ratio and the measured $\bar{K}_d(490)$ includes the variation introduced by changes in Sun angle. Applying the simple model of *Sathyendranath et al.* [1989] shows that for the same absorption and backscattering coefficients, $\bar{K}_d(490)$ can vary by 30% if the solar zenith angle varies between 20° and 70°. This source of variation affects the performance of both empirical algorithms for estimating $\bar{K}_d(490)$.

[26] In contrast to methods 1 and 2, method 3 (the semianalytical approach) produced much better results for all $\bar{K}_d(490)$ values, especially with substantial improvements for the values larger than 0.2 m^{-1} (see Figures 2c and 3c). There is no systematic over- or underestimation across the $\bar{K}_d(490)$ range, as indicated by the squared correlation coefficient of 0.91, intercept of 0.011 m^{-1}, and slope of 0.88 (Table 1). 90% of $\bar{K}_d^{\mathrm{der}}(490)$ derived by

method 3 fall within ±25% of $\bar{K}_d^{mea}(490)$ (see Figure 3c), and the average of absolute percentage difference (apd) is ~14% (Table 1). These results indicate significant improvements of method 3 over the empirical algorithms. Note that there was no tuning of the algorithm coefficients in the derivation of $\bar{K}_d(490)$ from $R_{rs}(\lambda)$ in the application of the semianalytical algorithm to the data set in this study. Also importantly, for the data from three different regions examined (see Figures 2c and 3c), the performance of method 3 shows no regional differences, although many of the data were from the Baltic which represents optically complex case 2 waters [*Darecki and Stramski*, 2004].

[27] It is necessary to emphasize that the standard case 1/case 2 classification of waters is not based on values of R_{rs} but rather on a qualitative aspect of covariation between chlorophyll and other optically significant constituents of water and their effects on optical properties [*Gordon and Morel*, 1983; *International Ocean-Color Coordinating Group*, 2000]. In literature, it is often assumed (or implied) that open ocean waters are case 1 while other waters (especially coastal) are case 2. Such a simplified separation is actually inconsistent with the case 1/case 2 definitions, and it can be incorrect. For example, open ocean waters can be either case 1 or case 2 [*Mobley et al.*, 2004]. Ideally, only waters whose optical properties are fully controlled by chlorophyll concentration (e.g., a pure phytoplankton culture) satisfy the original criteria of the definition of case 1 waters [*Morel and Prieur*, 1977]. In remote sensing of ocean color, the values of Chl and the optical properties of water are not known a priori, it is thus unclear if the water body under study meets the criteria for case 1 waters. Therefore uncertainties arise when algorithms designed for case 1 waters are applied to remotely sensed data. The robust and stable results from the semianalytical approach (method 3), however, clearly demonstrate an opportunity to overcome these uncertainties because the approach does not require any assumptions involved in the case 1/case 2 separation.

[28] The ~14% difference for method 3 is small given the fact that measurement errors in both R_{rs} and $\bar{K}_d$ as well as some approximations in the semianalytical derivation procedure cannot be avoided due to limitations in measurement methodology and the lack of unique relationships between the various optical properties in highly variable natural environments. For data with such a wide range of $\bar{K}_d(490)$ values (0.04–4.0 m^{-1}) including optically complex Baltic waters [*Darecki and Stramski*, 2004], the relatively small difference of 14% is encouraging and suggests a significant improvement in our ability to use ocean color remote sensing for monitoring important water properties. Our results show that the semianalytical method of deriving $\bar{K}_d(490)$ from R_{rs} is valuable because it provides $\bar{K}_d(490)$ estimates that are consistent with those obtained from in situ $E_d(z)$ measurements over a wide range of $\bar{K}_d(490)$ values. Note that $\bar{K}_d^{mea}$ is based on the vertical distribution of $E_d(z)$, while $\bar{K}_d^{der}$ is based on the spectral distribution of $R_{rs}(\lambda)$, so the sources of information for calculating $\bar{K}_d^{mea}$ and $\bar{K}_d^{der}$ are completely different.

[29] The better performance of method 3 compared to method 1 and method 2 is not so surprising because the semianalytical method is based on principles of radiative transfer and radiative transfer-based relationships between the various optical properties of the ocean. Although the approach involves some coefficients derived from numerical solutions of the radiative transfer equation [*Gordon*, 1989; *Lee et al.*, 2005], its application puts less restriction in terms of matching the data used for the algorithm development and the data of water bodies for which the $\bar{K}_d$ algorithm is applied. Thus better performance of this method can be expected, as demonstrated by Figures 2c and 3c. Method 3 reasonably corrects for the four limiting factors that appear in the empirical algorithms. Specifically, (1) method 3 is not a data-driven algorithm, so it has less dependence on the data themselves and their range; (2) method 3 uses $R_{rs}(\lambda)$ values, not simply the spectral ratios of $R_{rs}(\lambda)$; (3) a relatively long wavelength of light (640 nm) is introduced in the semianalytical approach, which increases its sensitivity and accuracy for estimating water properties in turbid waters, and widens the applicability of data collected by satellite sensors; and (4) the effect of Sun angle is accounted for in method 3, which provides more realistic estimates of $\bar{K}_d$, consistent with the character of an apparent optical property. As discussed above, these four limitations may deteriorate the performance of the standard empirical $\bar{K}_d(490)$ algorithms.

4.2. $\bar{K}_d(443)$

[30] As mentioned in Section 2, in method 1 $\bar{K}_d^{der}$ at 443 nm is empirically extrapolated from the method 1-derived $\bar{K}_d^{der}$ at 490 nm, following the approach of *Austin and Petzold* [1986], i.e.,

$$\bar{K}_d^{der}(443) = 0.0178 + 1.517\left(\bar{K}_d^{der}(490) - 0.016\right). \quad (9)$$

In method 2, $\bar{K}_d^{der}$ at 443 nm is calculated the same way as was done for $\bar{K}_d^{der}$ at 490 nm, with the only difference being the spectral values of $K_w(\lambda)$, $\chi(\lambda)$, and $e(\lambda)$ [*Morel and Maritorena*, 2001], which are 0.00885, 0.10963, and 0.6717, respectively. When applying methods 1 and 2 for the derivation of $\bar{K}_d(443)$, the model constants (such as 0.0178 m^{-1} and 1.517 in equation (9)) were those at 440 nm. We recognize that negligible errors may result from a 3 nm difference between 443 and 440 nm. Finally, in method 3, $\bar{K}_d(443)$ is calculated the same way as that for 490 nm, with the exception that the values of $a(443)$ and $b_b(443)$ are based on inversions of measured $R_{rs}(443)$, as indicated by *Lee et al.* [2002].

[31] Figure 4 compares $\bar{K}_d^{der}$ and $\bar{K}_d^{mea}$ at 443 nm, where $\bar{K}_d^{mea}$ is calculated from the vertical profiles of $E_d(443, z)$. For $\bar{K}_d^{mea}$ ranging from ~0.04 to 5.0 m^{-1}, $\bar{K}_d(443)$ derived by methods 1 and 2 again exhibits much larger differences between $\bar{K}_d^{der}$ and $\bar{K}_d^{mea}$ than found using method 3, especially for waters with larger $\bar{K}_d(443)$ values. As with $\bar{K}_d(490)$, method 1 underestimated $\bar{K}_d(443)$ on the higher end, and overestimated $\bar{K}_d(443)$ for lower $\bar{K}_d(443)$values ($\bar{K}_d(443) \equiv \bar{K}_d^{mea}(443) < 0.1$ m^{-1}). Method 2 significantly underestimated $\bar{K}_d(443)$ (about a factor of 2.5) at higher values ($\bar{K}_d(443) > 0.3$ m^{-1}). For lower values ($\bar{K}_d(443) <$ 0.1 m^{-1}), which are generally characteristic of blue oceanic waters, method 2 performed quite well. Method 3, again, performed well across the entire range of $\bar{K}_d(443)$ values (see Table 1 for quantitative evaluation of the three methods), which further supports the superiority of the semianalytical approach.

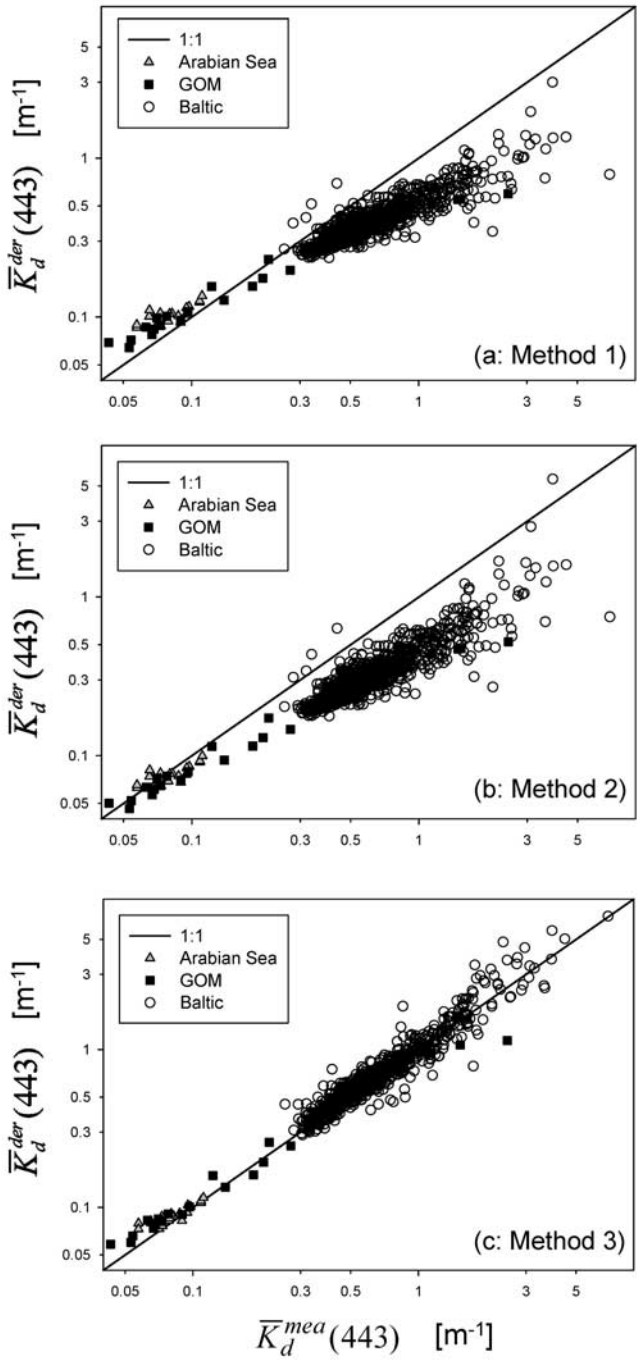

Figure 4. Same as Figure 2, but for 443 nm for (a) method 1, (b) method 2, and (c) method 3.

[32] We note that in the derivation of $\bar{K}_d(443)$ by both empirical methods there is no utilization of the values of R_{rs} (or L_w) actually measured at 443 nm. The application of both empirical methods relied on the ratio of $R_{rs}(490)/R_{rs}(555)$ to provide a result for 443 nm. Conceptually, such an approach is certainly less reliable than using data actually measured at a wavelength of interest (note a nearly 50 nm gap between 443 and 490 nm). In practice, the empirical algorithms for $\bar{K}_d(443)$ can be refined to incorporate R_{rs} (or L_w) measured at 443 nm. However, as discussed earlier, empirical algorithms will always face uncertainties associated with data consistency between derivation and application data sets. For obtaining reliable and accurate products from ocean color remote sensing, the use of semianalytical approaches may often be advantageous, as demonstrated by our results for method 3.

5. Conclusions

[33] We tested and compared various methods that derive the diffuse attenuation coefficient of downwelling irradiance from remote sensing reflectance using a large (N = 875) independent data set covering a range of natural waters from open ocean to turbid coastal areas. These methods include the current operational empirical algorithms used in conjunction with the SeaWiFS and MODIS satellite missions, and a newly developed semianalytical algorithm.

[34] For a wide range of $\bar{K}_d(490)$ values (0.04 to 4.0 m^{-1}) covered in this study, only 44% or so of the empirical algorithm-derived $\bar{K}_d(490)$ values fall within ±25% of the measured $\bar{K}_d(490)$ values derived from irradiance profiles. The empirical algorithms produced significant and systematic underestimation for $\bar{K}_d(490)$ values >0.2 m^{-1}. Similar results were also found for $\bar{K}_d(443)$. Many factors contributed to the rather poor performance of the two empirical algorithms. The main factor is likely the mismatch between the historical data used for the algorithm development and the data used in our study for algorithm evaluation which included more turbid coastal waters.

[35] The newly developed semianalytical algorithm (method 3) performed well over the entire range of $\bar{K}_d(490)$ and $\bar{K}_d(443)$ examined. Using method 3, over 90% of the derived $\bar{K}_d(490)$ are within ±25% of the measured values, and the average of absolute percentage difference between derived and measured values is ~14% for $\bar{K}_d(490)$ and ~11% for $\bar{K}_d(443)$. An important attribute of semianalytical approaches such as method 3 is that its application requires no separation of the entire data set into subsets of data, such as case 1 and case 2 waters that are often implied in current bio-optical analysis or modeling of ocean waters.

[36] Although more tests and evaluation analyses are necessary, the results presented in this study suggest that the semianalytical method 3 is a promising approach for estimating the diffuse attenuation coefficient from remote sensing reflectance. This method may be applied to satellite measurements of ocean color to provide consistent $\bar{K}_d$ data products over a wide range of optical water types within the world oceans. The computational efficiency of the semianalytical approach is about the same as that of empirical algorithms, so there is no computation time issue when processing large volumes of satellite data. Also, the good agreement between R_{rs}-derived $\bar{K}_d$ of method 3 and $E_d(z)$-calculated $\bar{K}_d$ values indicates that closure is achieved between the two independent methods of measurements and determinations that are both dependent on absorption and backscattering coefficients. Such a closure can be used as a quality check for R_{rs} and $\bar{K}_d$ data measured in the field by means of method 3.

Appendix A: Quasi-Analytical Algorithm (QAA) for Total Absorption Coefficient and Backscattering Coefficient

[37] The Quasi-Analytical Algorithm (QAA) [*Lee et al.*, 2002] starts with the calculation of the total absorption

coefficient (a) at a reference wavelength (λ_0, usually 555 or 640 nm). For instance, when 555 nm is selected as the reference wavelength (typically for open oceanic waters), $a(555)$ is calculated with

$$a(555) = 0.0596 + 0.2\,\left(a(440)_i - 0.01\right), \tag{A1}$$

where

$$a(440)_i = \exp\left(-1.8 - 1.4\nu + 0.2\nu^2\right) \tag{A2}$$

and $\nu = \ln(r_{rs}(440)/r_{rs}(555))$. Here $a(440)_i$ is an intermediate parameter for the derivation of $a(555)$.

[38] The "remote sensing" reflectance just below the surface is $r_{rs}(\lambda)$, and it relates to the above-surface remote sensing reflectance $R_{rs}(\lambda)$ through

$$r_{rs}(\lambda) = R_{rs}(\lambda)/(0.52 + 1.7\,R_{rs}(\lambda)). \tag{A3}$$

When r_{rs} at wavelength λ is known, the ratio of backscattering coefficient (b_b) to the sum of backscattering and absorption coefficients ($b_b/(a + b_b)$) at λ can be calculated algebraically based on the models of *Gordon et al.* [1988] and *Lee et al.* [1999]:

$$\frac{b_b}{a+b_b} = \frac{-0.0895 + \sqrt{(0.0895)^2 + 4 \times 0.1247\,r_{rs}}}{2 \times 0.1247}. \tag{A4}$$

[39] The spectral $b_b(\lambda)$ is modeled with the widely used expression [*Gordon and Morel*, 1983; *Smith and Baker*, 1981]

$$b_b(\lambda) = b_{bw}(\lambda) + b_{bp}(555)\left(\frac{555}{\lambda}\right)^{\eta}, \tag{A5}$$

where b_{bw} and b_{bp} are the backscattering coefficients of pure seawater and suspended particles, respectively. Values of $b_{bw}(\lambda)$ are provided in *Morel* [1974].

[40] When $a(555)$, the ratio of $b_b/(a + b_b)$ at 555 nm, and $b_{bw}(555)$ are known, $b_{bp}(555)$ in equation (A5) can be easily derived. The values of $b_b(\lambda)$ at other wavelengths are then calculated with the power parameter (η) estimated from [*Lee et al.*, 2002]

$$\eta = 2.2\,\left(1 - 1.2\,\exp\left(-0.9\frac{r_{rs}(440)}{r_{rs}(555)}\right)\right). \tag{A6}$$

Finally, by applying b_b to the ratio of $b_b/(a + b_b)$ derived from r_{rs} measured at wavelength λ (A4), the total absorption coefficient at λ, $a(\lambda)$, is calculated algebraically.

Appendix B: Semianalytical Model for Diffuse Attenuation Coefficient ($\bar{K}_d$)

[41] This $\bar{K}_d$ model [*Lee et al.*, 2005] is a refinement of that of *Sathyendranath et al.* [1989] where $\bar{K}_d$ is simply expressed as

$$\bar{K}_d = D_0(a + b_b), \tag{B1}$$

where $D_0 = 1/\cos(\theta_w)$ and θ_w is the solar zenith angle just below the surface.

[42] From analysis of the radiative transfer equation (RTE) and numerical simulations of the RTE, $\bar{K}_d$ in general has a form [*Lee et al.*, 2005]

$$\bar{K}_d = m_0\,a + \nu\,b_b, \tag{B2}$$

where the parameters m_0 and ν describe the contributions of a and b_b to $\bar{K}_d$, respectively. Theoretically and numerically, it was found that $m_0 \neq \nu$ [*Lee et al.*, 2005]. For different sun angles and different inherent optical properties of water, the value of ν can be three times greater than the value of m_0.

[43] On the basis of extensive numerical radiative transfer simulations with Hydrolight [*Mobley*, 1995], it was found that $m_0 \approx (1 + 0.005\,\theta_a)$ with θ_a the solar zenith angle above the surface, and ν can be expressed as [*Lee et al.*, 2005]

$$\nu = m_1(1 - m_2 e^{-m_3 a}), \tag{B3}$$

with values of m_1, m_2, and m_3 as 4.18, 0.52, and 10.8, respectively, for the surface layer. Because values of a and b_b can be adequately derived from remote sensing reflectance [*Hoge and Lyon*, 1996; *Lee et al.*, 2002; *Loisel et al.*, 2001], the value of $\bar{K}_d$ can then be estimated.

[44] **Acknowledgments.** Support for this study was provided by the Naval Research Laboratory's basic research P.E. 06010115N "Hyperspectral Characterization of the Coastal Zone" (NRL), the Polish National Committee for Scientific Research Grant PBZ-KBN 056/P04/2001 (M.D.), ONR contract N00014-02-1-0211 (K.L.C.), and NASA grants NAG-W10288 (NRL), NAS5-31716 (K.L.C.), and NAG5-12397 (D.S.). Z.P.L. is grateful to Cheng-Chien Liu of the National Cheng Kung University for discussions regarding the subject and to two anonymous reviewers for comments and suggestions.

References

Austin, R. W., and T. J. Petzold (1981), The determination of the diffuse attenuation coefficient of sea water using the coastal zone color scanner, in *Oceanography From Space*, edited by J. F. R. Gower, pp. 239–256, Springer, New York.

Austin, R. W., and T. J. Petzold (1986), Spectral dependence of the diffuse attenuation coefficient of light in ocean waters, *Opt. Eng.*, *25*, 473–479.

Carder, K. L., and R. G. Steward (1985), A remote-sensing reflectance model of a red tide dinoflagellate off West Florida, *Limnol. Oceanogr.*, *30*, 286–298.

Carder, K. L., F. R. Chen, Z. P. Lee, S. K. Hawes, and D. Kamykowski (1999), Semianalytic Moderate-Resolution Imaging Spectrometer algorithms for chlorophyll a and absorption with bio-optical domains based on nitrate-depletion temperatures, *J. Geophys. Res.*, *104*, 5403–5421.

Chang, G. C., and T. D. Dickey (2004), Coastal ocean optical influences on solar transmission and radiant heating rate, *J. Geophys. Res.*, *109*, C01020, doi:10.1029/2003JC001821.

Darecki, M., and D. Stramski (2004), An evaluation of MODIS and SeaWiFS bio-optical algorithms in the Baltic Sea, *Remote Sens. Environ.*, *89*, 326–350.

Du, K. P., Z. P. Lee, M. X. He, Z. S. Liu, and R. Arnone (2005), Angular variation of remote-sensing reflectance and the influence of particle phase functions, *Sci. China*, in press.

Gordon, H. R. (1989), Can the Lambert-Beer law be applied to the diffuse attenuation coefficient of ocean water?, *Limnol. Oceanogr.*, *34*, 1389–1409.

Gordon, H. R., and A. Morel (1983), *Remote Assessment of Ocean Color for Interpretation of Satellite Visible Imagery: A Review*, 44 pp., Springer, New York.

Gordon, H. R., O. B. Brown, and M. M. Jacobs (1975), Computed relationship between the inherent and apparent optical properties of a flat homogeneous ocean, *Appl. Opt.*, *14*, 417–427.

Gordon, H. R., O. B. Brown, R. H. Evans, J. W. Brown, R. C. Smith, K. S. Baker, and D. K. Clark (1988), A semi-analytic radiance model of ocean color, *J. Geophys. Res.*, *93*, 10,909–10,924.

Hoge, F. E., and P. E. Lyon (1996), Satellite retrieval of inherent optical properties by linear matrix inversion of oceanic radiance models: An analysis of model and radiance measurements errors, *J. Geophys. Res.*, *101*, 16,631–16,648.

International Ocean-Color Coordinating Group (2002), Remote sensing of ocean colour in coastal, and other optically-complex, waters, *Rep. 3*, edited by S. Sathyendranath, Dartmouth, Canada.

Jerlov, N. G. (1976), *Marine Optics*, Elsevier, New York.

Kirk, J. T. O. (1986), *Light and Photosynthesis in Aquatic Ecosystems*, Cambridge Univ. Press, New York.

Lee, Z. P., and K. L. Carder (2000), Band-ratio or spectral-curvature algorithms for satellite remote sensing?, *Appl. Opt.*, *39*, 4377–4380.

Lee, Z. P., K. L. Carder, T. G. Peacock, C. O. Davis, and J. L. Mueller (1996), Method to derive ocean absorption coefficients from remote-sensing reflectance, *Appl. Opt.*, *35*, 453–462.

Lee, Z. P., K. L. Carder, C. D. Mobley, R. G. Steward, and J. S. Patch (1999), Hyperspectral remote sensing for shallow waters: 2. Deriving bottom depths and water properties by optimization, *Appl. Opt.*, *38*, 3831–3843.

Lee, Z. P., K. L. Carder, and R. Arnone (2002), Deriving inherent optical properties from water color: A multi-band quasi-analytical algorithm for optically deep waters, *Appl. Opt.*, *41*, 5755–5772.

Lee, Z. P., K. L. Carder, and K. P. Du (2004), Effects of molecular and particle scatterings on model parameters for remote-sensing reflectance, *Appl. Opt.*, *43*, 4957–4964.

Lee, Z.-P., K.-P. Du, and R. Arnone (2005), A model for the diffuse attenuation coefficient of downwelling irradiance, *J. Geophys. Res.*, C02016, doi:10.1029/2004JC002275.

Lewis, M. R., M. Carr, G. Feldman, W. Esaias, and C. McMclain (1990), Influence of penetrating solar radiation on the heat budget of the equatorial pacific ocean, *Nature*, *347*, 543–545.

Liu, C.-C., K. L. Carder, R. L. Miller, and J. E. Ivey (2002), Fast and accurate model of underwater scalar irradiance, *Appl. Opt.*, *41*, 4962–4974.

Loisel, H., D. Stramski, B. G. Mitchell, F. Fell, V. Fournier-Sicre, B. Lemasle, and M. Babin (2001), Comparison of the ocean inherent optical properties obtained from measurements and inverse modeling, *Appl. Opt.*, *40*, 2384–2397.

Marra, J., C. Langdon, and C. A. Knudson (1995), Primary production, water column changes, and the demise of a Phaeocystis bloom at the Marine Light-Mixed Layers site (59°N, 21°W) in the northeast Atlantic Ocean, *J. Geophys. Res.*, *100*, 6633–6644.

McClain, C. R., K. Arrigo, K.-S. Tai, and D. Turk (1996), Observations and simulations of physical and biological processes at ocean weather station P, 1951–1980, *J. Geophys. Res.*, *101*, 3697–3713.

Mobley, C. D. (1995), Hydrolight 3.0 users' guide, report, SRI Int., Menlo Park, Calif.

Mobley, C. D., D. Stramski, W. P. Bissett, and E. Boss (2004), Optical modeling of ocean waters: Is the case 1-case 2 still useful?, *Oceanography*, *17*, 60–67.

Morel, A. (1974), Optical properties of pure water and pure sea water, in *Optical Aspects of Oceanography*, edited by N. G. Jerlov and E. S. Nielsen, pp. 1–24, Elsevier, New York.

Morel, A. (1988), Optical modeling of the upper ocean in relation to its biogenous matter content (case 1 waters), *J. Geophys. Res.*, *93*, 10,749–10,768.

Morel, A., and D. Antoine (1994), Heating rate within the upper ocean in relation to its bio-optical state, *J. Phys. Oceanogr.*, *24*, 1652–1665.

Morel, A., and B. Gentili (1993), Diffuse reflectance of oceanic waters: 2. Bi-directional aspects, *Appl. Opt.*, *32*, 6864–6879.

Morel, A., and S. Maritorena (2001), Bio-optical properties of oceanic waters: A reappraisal, *J. Geophys. Res.*, *106*, 7163–7180.

Morel, A., and L. Prieur (1977), Analysis of variations in ocean color, *Limnol. Oceanogr.*, *22*, 709–722.

Mueller, J. L. (2000), SeaWiFS algorithm for the diffuse attenuation coefficient, K(490), using water-leaving radiances at 490 and 555 nm, in *SeaWiFS Postlaunch Calibration and Validation Analyses*, part 3, edited by S. B. Hooker, pp. 24–27, NASA Goddard Space Flight Cent., Greenbelt, Md.

Mueller, J. L., and C. C. Trees (1997), Revised SeaWiFS prelaunch algorithm for diffuse attenuation coefficient K(490), *NASA Tech. Memo., TM-104566*, vol. 41, 18–21.

Mueller, J. L., C. Davis, R. Arnone, R. Frouin, K. L. Carder, Z. P. Lee, R. G. Steward, S. Hooker, C. D. Mobley, and S. McLean (2002), Above-water radiance and remote sensing reflectance measurement and analysis protocols, *NASA Tech. Mem., TM-2002-210004*, 171–182.

O'Reilly, J., S. Maritorena, B. G. Mitchell, D. Siegel, K. L. Carder, S. Garver, M. Kahru, and C. McClain (1998), Ocean color chlorophyll algorithms for SeaWiFS, *J. Geophys. Res.*, *103*, 24,937–24,953.

Platt, T., S. Sathyendranath, C. M. Caverhill, and M. Lewis (1988), Ocean primary production and available light: Further algorithms for remote sensing, *Deep Sea Res.*, *35*, 855–879.

Preisendorfer, R. W. (1976), *Hydrologic Optics*, vol. 1, *Introduction*, Natl. Tech. Inf. Serv., Springfield, Va.

Reynolds, R. A., D. Stramski, and B. G. Mitchell (2001), A chlorophyll-dependent semianalytical reflectance model derived from field measurements of absorption and backscattering coefficients within the Southern Ocean, *J. Geophys. Res.*, *106*, 7125–7138.

Sathyendranath, S., and T. Platt (1997), Analytic model of ocean color, *Appl. Opt.*, *36*, 2620–2629.

Sathyendranath, S., T. Platt, C. M. Caverhill, R. E. Warnock, and M. R. Lewis (1989), Remote sensing of oceanic primary production: Computations using a spectral model, *Deep Sea Res.*, *36*, 431–453.

Smith, R. C., and K. S. Baker (1981), Optical properties of the clearest natural waters, *Appl. Opt.*, *20*, 177–184.

Stramska, M., D. Stramski, R. Hapter, S. Kaczmarek, and J. Stón (2003), Bio-optical relationships and ocean color algorithms for the north polar region of the Atlantic, *J. Geophys. Res.*, *108*(C5), 3143, doi:10.1029/2001JC001195.

Zaneveld, J. R. V., J. C. Kitchen, and H. Pak (1981), The influence of optical water type on the heating rate of a constant depth mixed layer, *J. Geophys. Res.*, *86*, 6426–6428.

K. L. Carder, College of Marine Science, University of South Florida, St. Petersburg, FL 33701, USA. (kcarder@marine.usf.edu)

M. Darecki, Institute of Oceanology, Polish Academy of Sciences, Powstancow Warszawy 55, 81-712 Sopot, Poland. (darecki@iopan.gda.pl)

C. O. Davis and W. J. Rhea, Naval Research Laboratory, Code 7203, Washington, DC 20375, USA. (davis@rira.rl.navy.mil; rhea@nrl.navy.mil)

Z.-P. Lee, Naval Research Laboratory, Code 7333, Stennis Space Center, MS 39529, USA. (zplee@nrlssc.navy.mil)

D. Stramski, Marine Physical Laboratory, Scripps Institution of Oceanography, University of California at San Diego, La Jolla, CA 92093-0238, USA. (stramski@mpl.ucsd.edu)